中國機械工程學刊第四十卷第六期第 711~717 頁(民國一百零八年)
Journal of the Chinese Society of Mechanical Engineers, Vol.40, No.6, pp 711~717 (2019)

Effect of Square Wave Tool Path Pattern on Mechanical and Microstructure Properties of Friction Stir Welded AA6061-Cu Dissimilar Alloys

D. Jayabalakrishnan * and M. Balasubramanian**

Keywords: Friction stir welding; Pin profile; Square wave Pattern; X-ray; Microstructure.

ABSTRACT

In this present work friction stir welding of Al 6061-annealed pure copper dissimilar metals with square wave pattern tool pin movement was investigated. The aim of this experiment is to identify the significance square wave tool movement on friction stir welding process along with three different tool pin profiles. Different tool pin profiles of square, round and spiral shapes were selected and their significant outcomes were unveiled. Friction stir welding process parameters of 1500 and 2000 rpm & tool pin movement step size of 1.0 mm and 2.0 mm & weaving rate of 100 mm/min and 150mm/min were selected. The advantages of tool movement pattern and tool pin profile shape were examined by mechanical testing, micro-structure analysis and energy dispersive X-ray analysis. The mechanical results were showed that process parameter of 1500 rpm, 1.0 mm step size, weaving rate of 150 mm/min and square tool pin profile combination gives better mechanical properties. Micro structural results unveiled achievement of better grain refinement and uniform dispersion of micro constituents by implementation of square wave tool pin movement pattern along with square tool pin profile. X-ray radiography results revealed defect free nature of weldments. The EDAX report confirms that the weld nugget contains both aluminium and copper as equal percentage, which indicates fine mixing of two parent metals.

Paper Received August, 2017. Revised August, 2018. Accepted October, 2018.Author for Correspondence: D. Jayabalakrishnan

**Assistant Professor, Department of Mechanical Engineering, Sriram Engineering College, Chennai, India*

***Professor, Department of Mechanical Engineering, RMK College of Engineering and Technology, Chennai, India*

** djayabal2001@gmail.com*
manianmb@gmail.com

INTRODUCTION

Friction stir welding is a pollution free, solid-state welding technique where metals are joined using frictional heat and pressure (Shen and Liu 2010; Vijayan et al, 2010). A rotating tool rotates over a specimen at desired rpm due to that frictional heat develops and metal gets plasticize. The plasticized metals are joined with each other with the help of pressure. The need for lightweight aluminium products in aircraft industries, automobile and construction areas is increasing day by day. The Automobile sector is attempting to replace iron products with lightweight aluminium to improve their product efficiency. Joining non-ferrous metals using friction stir welding process is the foremost method where similar and dissimilar metals joining and energy saving process parameters are highly welcome phenomenon nowadays. The weld quality in FSW process depends greatly on the work piece metal, weaving speed, tool rotation rpm and degree of intermixing of parent metals (Khan et al, 2015; Rodriguez et al, 2015). Tool pin movement could play a vital role in complete intermixing of parent metal which it could be directly proportional to strength of weldments. Welding of similar alloys has a low degree of complexity whereas it is not so with welding of dissimilar alloys due to mismatch of the cooling rate Mahto et al, (2016). In higher melting temperature, metal cool rapidly than lower melting temperature and thus requiring special parameters. High frictional heat at lower speed fetches good quality weldments with low energy consumption. Generally, in FSW, the tool rotates itself and moves in a straight line path, whereas in a square wave pattern method, the tool moves in both x-y directions thus making intermixing of parent metals possible. With complete intermixing of parent metals, the micro constituents are also dispersed throughout the matrix. This enables improvement of mechanical properties through precipitated strengthening (Mohammadi et al, 2015; Babu et al, 2009). The fine intermixing of parent metals could be achieved by tool face profile also. Hence, round, square and spiral tool pin profiles could be used as stir tools. Zhang et al, (2015) have confirmed that the dissimilar metals which are formed by friction stir welding produce tensile strength better than with aluminium base metal. They also indicate the formation of micro elements like Al_4Cu_9 and Al_2Cu on the nugget as a result of short circuit cooling. Bisadi.et.al, (2013) reported the dissimilar friction stir welding process parameters for aluminium and copper. They suggested that weldment was in good condition at lower tool rotation speeds, whereas defects developed when tool speed increased. The later was due to improper fusion and cooling.

EXPERIMENTAL METHODS

2.1 Materials

The aluminium used for this study was AA6061 (150mmx150mm) which contains 0.9% Mg, 0.62% Si, 0.28% Cu, 0.17% Cr, 0.33% Fe, 0.02% Zn, 0.06% Mn, 0.02% Ti and remaining was Al. The copper material used for this study was annealed pure copper. Table 1 shows the mechanical properties of parent metals. The tool material used for this study was HSS.

Table 1. Mechanical property of work piece materials

S. No	Material	Tensile strength (MPa)	Elongation (%)	Izod Impact (J)	Micro Hardness (Hv)
1	AA 6061	280	15	18	105
2	Copper	220	25	26	73

2.2 Procedure

Square shaped 6mm thick sheets of AA6061 and Copper were placed on the work bed as a butt joint configuration in a vertical milling centre with the help of mechanical clamps. Figure 1(c) shows the mechanical clamping of Al-Cu dissimilar metal plates. Machining was started at one end with process parameters. Figure 1(a) showed the experimental setup with tools. Figure 1(b) shows FSW tool pin profile with dimensions. It was noted that the difference in pin diameter and shoulder diameter was noted as 4mm; this is for reducing the width of weld bead. The Figure 2 (a) shows the different step sizes of tool movement pattern. A constant axial load of 6KN was applied throughout the process. Welding was performed with three different tool pin profiles. The welded samples were inspected for visual defects after completion of the post cleaning process.

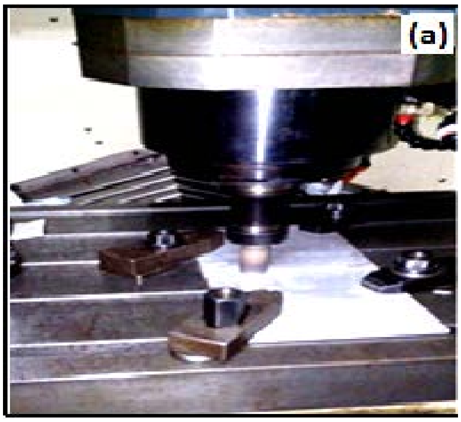

Figure 1 (a) FSW setup on VMC

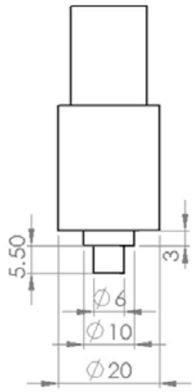

Figure 1 (b) FSW tool dimensions

Figure 1 (c) Mechanical clamping of Al-Cu plates on VMC

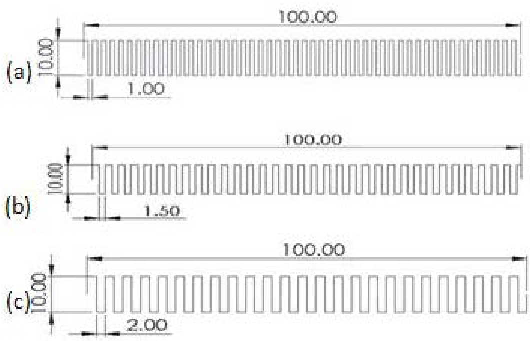

Figure 2 (a) Step sizes of tool pin movement patters

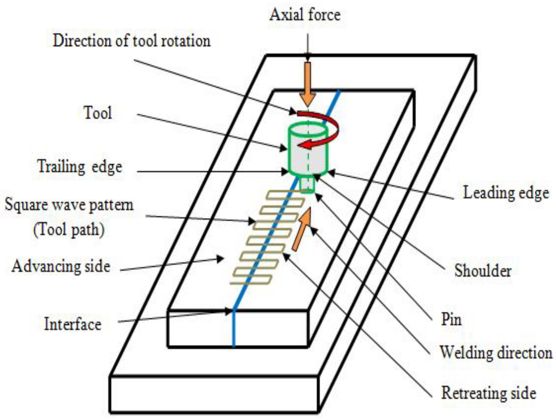

Figure 2 (b) schematic diagram of square wave tool pin movement pattern.

2.3 Specimen preparation

The cleaned welded components were cut based on ASTM standards for conducting various tests. Specimens were cut in required dimensions using abrasive water jet machine with nozzle diameter of 1mm, garnet size of 80 Mesh; flow rate of 0.35 Kg/min, maximum pressure of 320 MPa. The sectioned specimens were checked for dimensional accuracy before testing.

2.4 General Characterization

2.4.1 Mechanical characterization

The tensile strength of welded components was tested on the basis of ASTM E8M-04. A universal testing machine (MTS C44, India), 40 Ton of capacity with cross head speed of 1.5 mm/min was utilized for estimating the tensile properties of the welded samples. Tensile specimens were maintained with gauge length of 50mm and width of 12.5 mm. The notch tensile test was performed on the basis of ASTM E23. Five identical specimens were tested for each property and average values were computed. The Izod impact values of welded components were tested on the basis of ASTM 256 with Izod impact tester (Kristal, India) having 30 Joules of capacity. The micro hardness of different welded samples was measured according to ASTM 384 with a Vickers hardness tester.

2.4.2 Optical microscopy

Evaluation of the Welded portion microstructure was done by an optical microscope (Moticam 1000, China) having 25X lens zooming capacity. The specimens were cut by sawing process with cooling water attached for maintaining low temperature on the cutting zone and to avoid grain refinement. The sectioned specimens were mounted by thermosetting resin for effective edge retention. Mounted specimens were ground using an automated device which consisted of SiC abrasive sheet. The specimens were ground using a series of abrasive sheets of grit sizes ranging from 60 to 5/0 (US system). It is a kind of power sanding sheet contained coarse aluminium oxide abrasive particles in the size range of 60 µm for heavy polishing metal surfaces and removing small imperfections. The grades usually mention the particle size and the grain size. The aluminium oxide containing grit was chosen for the following advantages. They are self-renewing, long lasting and economical product. Mirror polishing was done by diamond fine abrasives followed by colloidal alumina paste. Potassium Dichromate and Keller solution were used as etching agents to reveal the grain structure of aluminium alloy. Finally, the specimen surface was cleaned using distilled water and all the micrograph images were taken in polarized light.

RESULTS & DISCUSSION

3.1 Mechanical properties

Table 2-4 shows the values of tensile, notch tensile, Izod impact and hardness of weld beads. The strength factor of weldments was calculated as keeping large value as 100% in all parameter and the percentage of other values were measured with the larger one by taking the ratio. The tensile values were improved significantly for the square wave tool pin movement pattern. Weld was done by 1500 rpm, 1mm step size and 150 mm/min weaving rate and square tool pin profile giving the maximum strength factor of 99.82 which is larger than with other process parameter weldments. This is because of the complete mixing of two parent metals since the tool rotates for a longer time in the welding zone. When the tool moves in both x and y directions; metal from the advancing side (copper) and the retreating side (aluminium) gets a complete mix. Hence inter metallic compounds like Mg, Si, Cr and Fe from aluminium were dispersed throughout the weld nugget. Similarly, fusion of parent metals generated Al_4Cu_9 and Al_2Cu phases. Formation of many secondary phases on matrix may arrest the crack propagation by poly phase strengthening method (Ghosh et al, 2011; Saeid et al, 2010). Similarly, when axial load was applied the precipitated inter- metallic compounds arrest the minute crack propagation through grain boundaries. These phenomena help the metal to bear a maximum load Mohanty et al, (2012). At lower tool rotation (1500rpm) the grains are processed in a gentle manner and do not get affected by heat. Thus, the rate of creation of heat-affected zones was minimum Chen et al, (2009). Maximum strength factor was achieved at a lower step size (1.0 mm) of the tool movement. This is because of the maximum number of turns can completed by the tool before it completes the full length of weld on plate. A fine mixture of parent metals reduces weld defects, improper mixing and poor cooling rate.

Thus the weld nuggets which were formed based on parameter 1500rpm, 1.0mm step size, 150mm weaving rate and square tool pin profile shows distinct results compared to other combinations. Figure 3(A) shows tensile specimens based on the ASTM standard. Figure 3(B) shows broken tensile specimens after the tensile test. The presence of some dimple portions was observed indicating a small persistence of brittleness from the nugget due to the thermally affected grains during the joining process. The Figure 4 (a-c) shows micro hardness values on the welded portion. It was noted that the maximum micro hardness of 81Hv was achieved on nugget zone for 2000 rpm, 1.0mm step size and 150mm/min weaving rate with square tool pin profile FSW. Grains were thermally affected at higher tool rotational speeds with increased brittleness improving the hardness. Grains were refined at the nugget and cooling was slow, which forms very finer grain size and improved the hardness. A relatively low hardness was seen on the advancing side as a result of coarse grain formation (Hu et.al, 2015; Xue et.al, 2010).

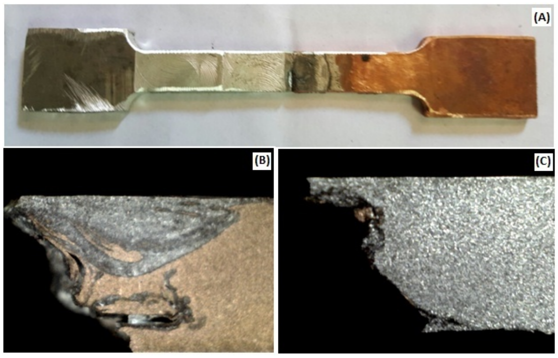

Figure 3 (A) ASTM tensile specimen (B) brittle fracture on advancing side and (C) fracture on retreating side

Table 2 Mechanical properties of Al 6061-Cu with round tool pin profile

Rotation speed/SS/ weaving rate	Tensile strength (MPa)	Normalized tensile strength (MPa) %	Notch tensile strength (MPa)	Normalized notch tensile strength (MPa) %	Yield strength (MPa)	Normalized yield strength (MPa) %	Impact strength (J)	Normalized impact strength (J) %	Strength Factor %
1500/ 1.0/100	196	99.5	167	98.8	136	96.5	7.6	93.8	97.15
1500/ 1.0/150	194	98.5	169	100	132	93.6	7.9	97.5	97.42
1500/ 2.0/100	191	97.0	161	95.2	135	95.7	8.1	100	96.97
1500/ 2.0/150	195	99.9	164	97.0	138	97.8	8.1	100	98.67
2000/ 1.0/100	189	96.0	165	97.6	141	100	7.8	96.2	97.45
2000/ 1.0/150	197	100	165	98.8	136	96.4	7.5	92.5	96.92
2000/ 2.0/100	190	96.4	164	97.0	134	95.0	7.9	97.5	96.47
2000/ 2.0/150	189	96.0	167	98.8	132	93.6	8.0	98.7	96.77

Table 3 Mechanical properties of Al 6061-Cu with square tool pin profile

Rotation speed/SS/ weaving rate	Tensile strength (MPa)	Normalized tensile strength (MPa) %	Notch tensile strength (MPa)	Normalized notch tensile strength (MPa) %	Yield strength (MPa)	Normalized yield strength (MPa) %	Impact strength (J)	Normalized impact strength (J) %	Strength Factor %
1500/ 1.0/100	199	92.9	168	96.5	139	100	7.9	94.0	95.85
1500/ 1.0/150	214	100	174	100	138	99.3	8.4	100	99.82
1500/ 2.0/100	196	91.6	166	95.4	135	97.1	8.0	95.2	94.82
1500/ 2.0/150	199	93.0	169	97.1	136	97.8	8.2	97.6	96.37
2000/ 1.0/100	195	91.1	167	95.6	139	100	7.7	91.6	94.57
2000/ 1.0/150	197	92.0	163	93.6	138	99.2	7.8	92.8	94.40
2000/ 2.0/100	196	91.6	168	96.5	136	97.8	7.9	94.0	95.00
2000/ 2.0/150	191	82.2	167	95.9	135	97.1	8.1	96.4	93.00

Table 4 Mechanical properties of Al 6061-Cu with spiral tool pin profile

Rotation speed/SS/ weaving rate	Tensile strength (MPa)	Normalized tensile strength (MPa) %	Notch tensile strength (MPa)	Normalized notch tensile strength (MPa) %	Yield strength (MPa)	Normalized yield strength (MPa) %	Impact strength (J)	Normalized impact strength (J) %	Strength Factor %
1500/ 1.0/100	198	100	165	97.0	134	95.7	7.5	92.5	96.3
1500/ 1.0/150	197	99.5	170	100	136	97.1	7.7	95.0	97.9
1500/ 2.0/100	194	97.9	165	97.0	135	96.4	8.0	98.7	97.5
1500/ 2.0/150	192	96.9	167	98.2	136	97.1	7.8	96.3	97.1
2000/ 1.0/100	189	95.5	162	95.3	140	100	7.4	91.3	95.5
2000/ 1.0/150	190	95.9	161	94.7	137	97.8	7.6	93.8	95.5
2000/ 2.0/100	188	94.9	163	95.9	138	98.5	7.9	97.5	96.7
2000/ 2.0/150	189	95.4	163	95.9	136	97.1	8.1	100	97.1

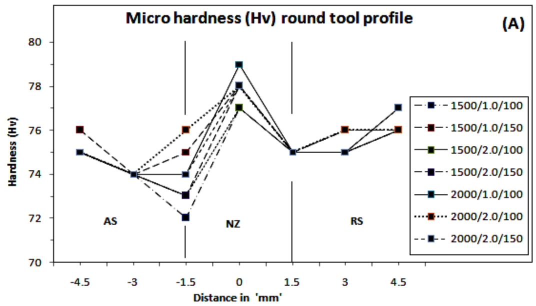

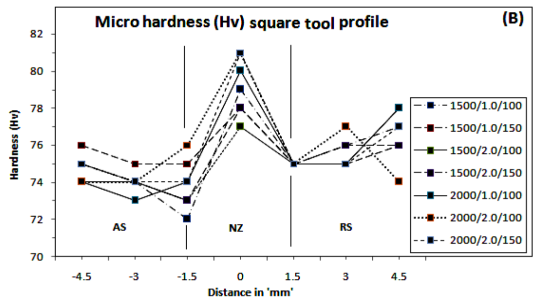

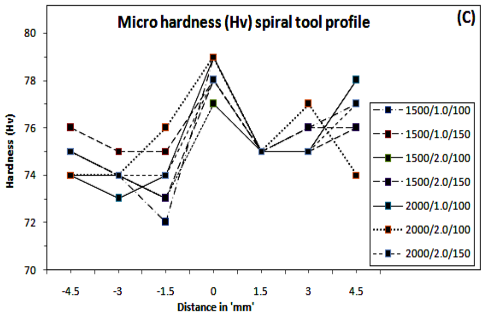

Figure 4 Micro hardness values of (a) round tool pin profile, (b) square tool pin profile and (c) spiral tool pin profile

3.2 Microstructure of joints

Figure 5 (a) shows a cross section microstructure of weldments which are formed with square wave tool pin movement and process parameters of 1500rpm, 1.0mm step size and 150mm/min weaving rate along with square tool pin profile. Figure 5(a) also shows the microstructure of the AA 6061 parent metal. Particles of eutectics were seen along the direction of tool. The fine particles are eutectics of Mg_2Si which were spread over the weld nugget, improving the load bearing capability. Uniform spread up was achieved as a result of square wave path of tool movement on the processed zone. The x-y traverse movement of tool enabled the complete mixing up of parent metals with each other. Figure 5(b) shows the field near the processed zone with large particles of Mg_2Si in primary aluminium alloy matrix Luis trueba et al, (2015). Figure 5(c) shows the interface junction of the parent metal with severely heated and recrystallized larger grain of primary aluminium with eutectics at the grain boundaries. Figure 5(d) shows another field with HAZ of base metal and the rapidly plasticized and cooled matrix of AA 6061. It reveals the brittleness of the nugget zone compared to other places. Hence a greater hardness was experienced. Figure 5(e) shows the rapidly plasticized and cooled zones with scripts of Al-Si and Mg2Si. The micro constituents were seen spread over the weld nugget zone and increased the load bearing capacity of weld nugget via precipitated strengthening (Shigematsu et al., 2003; Karthikeyan et al 2010). Figure 5(f) indicates the interface junctions of the fused zone as well as the melted zone of aluminium and copper HAZ. The fused zone was dark in colour with the constituents of both copper and AA6061 indicating a fine mixture of base metals. The copper zone showed completely dissolved grains of alpha and fine beta phase. Figure 5(g) shows the interface of parent metal copper and HAZ of copper. Partial recrystallization of copper solid solution was observed. Figures (h and i) show grains of copper near the HAZ with larger grains of copper solid solution due to grain growth. This is because high thermally affected grains took a larger time to cool. Hence the grains were grown as bigger one. The images (h and i) were the microstructure of the copper base metal from the HAZ and towards the unaffected zone. Thus it could be stated that the formation of fine mixture of aluminium and copper on the weld nugget zone was from microstructure images as a result of complete mixing via the square wave pattern. The square tool pin profile influenced the base metals to mix completely due to orthogonal stirring. When tool geometry is perpendicular to the work piece material, the contact area and the coefficient of friction on metal are on the higher side. This phenomenon helps the processed zone grains to be reoriented and mixed thoroughly on weldments (Joswik et al, 2001; Pruncu et al, 2015). Figure 6 shows x-ray radiography results of dissimilar aluminium and copper. Images 6 (a and b) show there was no weld flaw within the weldment portion indicating fine and uniform grain formation and proper cooling (Xue et al., 2010; Liu et al., 2011).

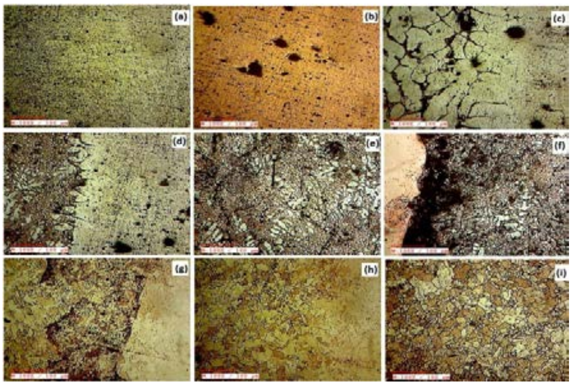

Figure 5 (a-i) Microstructure of weld nugget zones

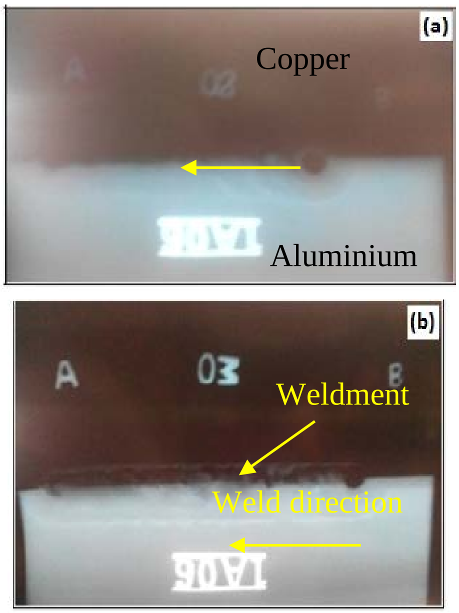

Figure 6 (a and b) X-ray radiography images of Al-Cu dissimilar weldments

3.3 Energy dispersive spectra analysis

Figure 7 (a-c) shows the EDAX analysis on the advancing side, nugget zone and retreating side of processed zones. The inference is that the advancing side has grains of primary aluminium whereas a nugget zone has a eutectic mixture of both aluminium and copper base metals. Similarly, the retreating side has grains of copper indicating complete fusion of two parent metals at the nugget with the formation of new crystals of both Al and Cu. Figure 7 (a) shows EDAX report on retreating side. It shows the presence of raw aluminium on the retreating side indicating the absence of copper. Figure 7 (b) shows the EDAX report on nugget with both aluminium (45%) and copper (35%) while the remaining were oxides of Al and Cu. The micro constituents were dispersed throughout the nugget zone. The oxide formation was due to heavy heat dissipation during machining. Similarly, 7(c) shows raw copper on advancing side.

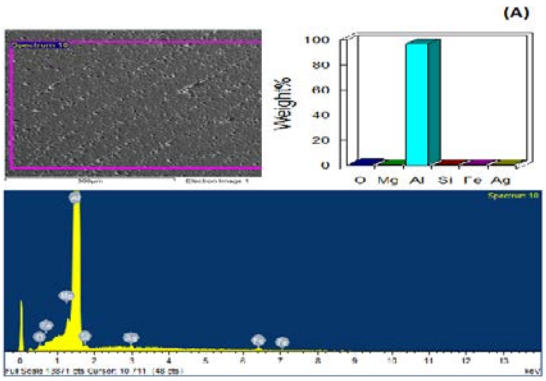

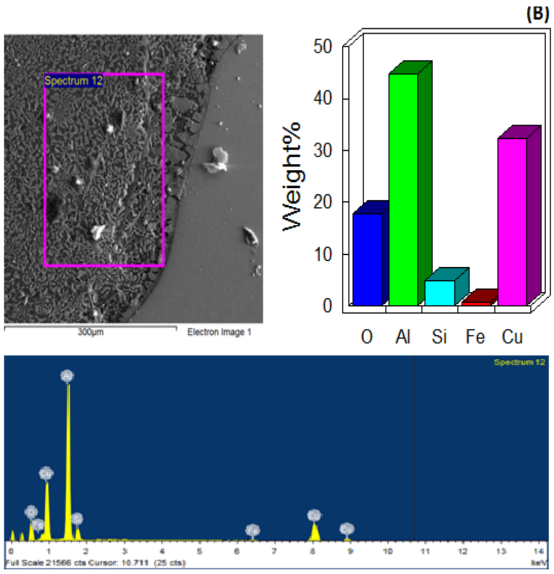

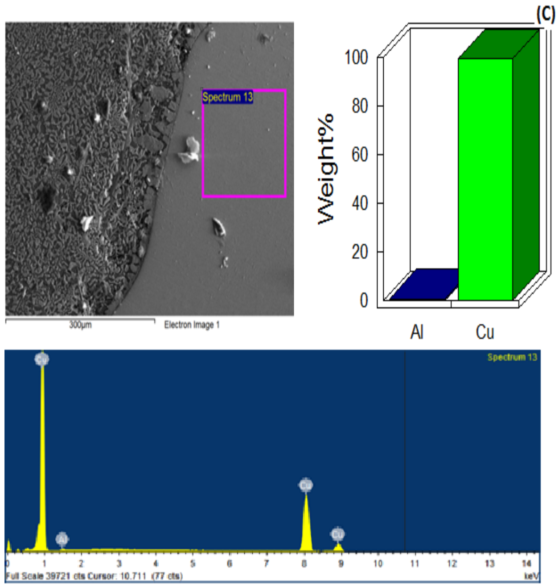

Figure 7 shows EDAX reports of (a) retreating side, (b) nugget zone and (c) advancing side of processed zone

CONCLUSIONS

The results obtained lead to the following conclusions. Square wave tool path pattern can be successfully implemented and welding can be done with different parameters. The process parameters of 1500 rpm, 1mm Step size and 150mm/min weaving rate along with square tool pin profile fetch the highest strength factor compare to other process parameters. The microstructure images reveal uniform grain flow and an even dispersion of micro constituents in all directions. The square wave tool pin pattern made weldments are defect free due to complete mixing of the parent metals and offer a uniform cooling. X-ray radiography results shows flaw free weldment of aluminium copper dissimilar metals. The EDAX analysis reveals the presence of grains of both copper and aluminium at the nugget. Hence square wave tool pin moving pattern method on friction stir welding fetches useful results in both mechanical and microstructure of welded AA6061-Cu alloy system. The refined process parameters of 1500rpm, 1mm step size (x-y tool movement) and 150mm/min weaving rate could be considered for better weldment qualities.

REFERENCES

Babu, S., Elangovan, K., Balasubramanian, V., Balasubramanian, M., “Optimizing Friction Stir Welding Parameters to Maximize Tensile Strength of AA2219 Aluminum Alloy Joints,” *Met. Mater Int*, Vol. 15, No. 2, pp. 321-330 (2009).

Chen, Y.C, Nakata, K., “Micro structural characterization and mechanical properties in friction stir welding of aluminum and titanium dissimilar alloys,” *Mater Des,* Vol 30, No.3, pp.469–474 (2009).

Ghosh, M., Kumar, K., Mishra, R.S., “Friction stir lap welded advanced high strength steels: microstructure and mechanical properties,” *Mater Sci Eng A*., Vol.528, No. 28, pp.8111–8119 (2011).

Bisadi, H., Tavakoli, A., Tour Sangsaraki, M., Tour Sangsaraki, K., “The influences of rotational and welding speeds on microstructures and mechanical properties of friction stir welded Al5083 and commercially pure copper sheets lap joints” *Mater Des*., Vol.43, pp.80-88 (2013)

Hu, Z.L., Wang, X.S., Pang, Q., Huang, F., Qin, X.P., Hua, L., “The effect of post processing on tensile property and microstructure evolution of friction stir welding aluminium alloy joint,” *Mater Char*.,Vol. 99,pp. 180-187 (2015).

Joswik, P., “Experimental Analysis of Crack Growth in a Notched Specimen Made of Ni3Al Inter Metallic Alloy,” *J. notch effect fracture*., Vol.11, pp.257-269(2001).

Karthikeyan, L., Senthilkumar, V.S, Padmanabhan, K.A., “On the role of process variables in the friction stir processing of cast aluminium A319 alloy,” *Mater. Des*., Vol. 31, pp.761–71 (2010).

Khan., Noor Zaman, Khan., Zahid, A., Siddiquee, Arshad Noor., “Effect of shoulder diameter to pin diameter (D/d) ratio on tensile strength of friction stir welded 6063 aluminium alloy,” *Mater.Today: Proceedings*., Vol.2, No. (4-5), pp.1450-1457(2015).

Liu, H.J., Shen, J. J., Zhou, L., Zhao, Y. Q., Liu. C., Kuang, L Y., “Micro structural characterization and mechanical properties of friction stir welded joints of aluminum alloy to copper,” *J. Sci. Technol. Weld. Join*., Vol.16, pp.92−99(2011).

Luis trueba, Jr., Georgiana Heredia., Lucie, B., Johannes., “Effect of tool shoulder features on defects and tensile properties of friction stir welded aluminium 6061-T6, *J. Mater. Proc. Technol*., Vol.12, pp.455-561(2015).

Mahto., Raju Prasad., Bhoje., Rahul, Pal., Surjya, K., Joshi., Harshadeep, S., Das., Siddhartha., “A study on mechanical properties in friction stir lap welding of AA 6061-T6 and AISI 304”, *Mat. Sci. Eng.A*., Vol.652, pp. 136-144(2016).

Mohammadi, J., Behnamian, Y., Mostafaei, A., Izadi, H., Saeid, T., Kokabi, A.H., Gerlich, A.P., “Materials Characterization Friction stir welding joint of dissimilar materials between AZ31B magnesium and 6061 aluminum alloys: Microstructure studies and mechanical characterizations,” *Mater. Char*., Vol.101, pp.189-20(2015).

Mohanty, H.K., Mahapatra, M.M., Kumar, P., Biswas, P., Mandal, N.R., “Modeling the effect of tool shoulder and probe profile geometries on friction stirred aluminum welds using RSM”, *J. Marine Sci. Appl*., Vol.11, pp.493-503 (2012).

Pruncu, C.I., Azari, Z., Casavola, C., “Characterization and prediction of cracks in coated materials,” *Int. sch. res. notice*. 594147, pp. 197-207. (2015).

Qiu-zheng zhang., Wen-biao., Gong., Wei Liu., “Microstructure and mechanical properties of dissimilar Al−Cu joints by friction stir welding,” *Trans. Nonferrous Met. Soc. China*., Vol.25, pp.1779−1786 (2015).

Rodriguez, R.I., Jordon, J.B., Allison, P.G., Rushing, T., Garcia, L., “Microstructure and mechanical properties of dissimilar friction stir welding of 6061-to-7050 aluminum alloys”, *Mater. Des*., Vol.83, pp.60-65 (2015).

Saeid, T, Abdollah-zadeh, A., Sazgari, B., “Weldability and mechanical properties of dissimilar aluminum–copper lap joints made by friction stir welding,” *J. Alloys Compd*., Vol.5, pp.490:652 (2010).

Shen, s.h, and Liu, H.J., “Effect of welding speed on microstructure and mechanical properties of friction stir welded copper,” *Mater. Des*, Vol.3, pp.3937–942(2010).

Shigematsu, I., Kwon, Y.J., Suzuki, K., Imai, T., Saito, N., “Joining of 5083 and 6061aluminum alloys by friction stir welding,” *J. Mater. Sci. lett*., Vol.22, pp.353–356 (2003).

Vijayan, S., Raju, R., Rao, S.R.K., “Multi objective optimization of friction stir welding process parameters on aluminum alloy AA 5083 using Taguchi-based grey relation analysis,” *Mater. Manuf. Process*., Vol.25, pp.1206–1212(2010).

Xue, E.P., Xiao, B.L., Ni, D.R, Mazy., “Enhanced mechanical properties of friction stir welded dissimilar Al−Cu joint by inter metallic compounds,” *J. Mater. Sci.Eng. A*, Vol.527, pp.5723−5727 (2010).

Xue, P., Xie, G.M., Xiao. B.L., Ma, Z.Y., Geng, L., “Effect of heat input conditions on microstructure and mechanical properties of friction-stir-welded pure copper,” *Metall Mater Trans A*., Vol.41, pp.2010–2021.(2010).